Geoderma 462 (2025) 117526

Contents lists available at ScienceDirect

Geoderma

journal homepage: www.elsevier.com/locate/geoderma

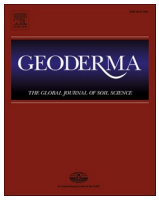

Soil total phosphorus content is a driver of P forms in continuously flooded paddy soils

Sara Martinengo [a,*], Lia Chilà [a,b], Martina Mazzon [c], Barbara Cade-Menun [d], Simone Bordignon [b], Roberto Gobetto [b], Maria Martin [a], Veronica Santoro [a], Luisella Celi [a]

[a] Department of Agricultural, Forest and Food Sciences, University of Turin, Italy
[b] Department of Chemistry, University of Turin, Italy
[c] Department of Agricultural and Food Sciences, Alma Mater Studiorum-University of Bologna, Italy
[d] Agriculture and Agri-Food Canada, Swift Current Research and Development Centre, Swift Current, SK, Canada

ARTICLE INFO

Handling Editor: Dr. Andrew Margenot

Keywords:
Rice
Paddy soil
Organic phosphorus compounds
Chemical fractionation
P-NMR

ABSTRACT

Redox fluctuations in submerged paddy soils strongly influence the transformation and availability of inorganic (P_i) and organic phosphorus (P_o) forms. However, the extent to which these redox-driven processes affect P_i and P_o pools and speciation, and their contribution to phosphorus (P) availability for rice, remains poorly understood.

This study examined P_i and P_o dynamics in twelve paddy soils with different total P (TP) content, classified as high-P (>800 mg P kg^{-1}), medium-P (500–800 mg P kg^{-1}), and low-P (<500 mg P kg^{-1}). Soils were analysed before and after 60 days of rice growth using sequential P fractionation, liquid-state ^{31}P nuclear magnetic resonance (^{31}P NMR) spectroscopy, and phosphomonoesterase activity assays to assess P pools (soluble, exchangeable, redox-sensitive, and residual), organic P composition, and enzymatic hydrolysis potential.

Redox-sensitive P_i and P_o were the dominant pools across all soils, accounting for ~50 % and ~18 % of total P, respectively. Soluble and exchangeable P pools remained minor. Concentrations of P_i and P_o were highest in high-P soils and lowest in low-P soils. In high-P soils, orthophosphate monoesters dominated and remained quite stable during plant growth, likely due to selective accumulation of inositol phosphates under repeated Fe redox cycles. In contrast, orthophosphate diesters in medium- and low-P soils represented the most labile component of P_o and were rapidly hydrolyzed during rice growth to alleviate P limitation.

These findings highlight how TP content modulates the contribution of P_i and P_o pools to rice nutrition, emphasizing the need to account for P_o dynamics when evaluating P availability in paddy systems under fluctuating redox conditions.

1. Introduction

Phosphorus (P) is an essential element for plants; however, owing to its strong affinity with soil constituents, phosphate is considered the most inaccessible nutrient for plant uptake in the majority of agricultural soils (Frossard et al., 2000). Combining that with the increasing demand of agricultural production, P has received increasing attention in the past decade over the long-term availability of rock phosphate, a nonrenewable resource used to produce chemical P fertilizers. This has shifted focus from fertilizer P to soil "legacy P" (Zhu et al., 2018), the supply of previously applied P fertilizer that has accumulated in the soil, and which is not immediately available for plant uptake (Solangi et al., 2023). Legacy P has mostly referred to phosphate, whereas less attention has been posed to the total soil P content, which in turn is characterized by various inorganic (P_i) and organic (P_o) P compounds. The former are mostly represented by phosphate (HPO_4^{2-} or $H_2PO_4^-$ at typical soil pH ranges), while the latter are divided into the compound classes orthophosphate monoesters, orthophosphate diesters, and phosphonates, based on the bond of phosphate to carbon (C) groups. Orthophosphate monoesters include sugar phosphates (i.e. glucose 6-phosphate),

Abbreviations: Ac-PME, acid phosphomonoesterase; Alk-PME, alkaline phosphomonoesterase; exchange-P, exchangeable P compounds; Fe-P, iron-bounded P compounds; Fe_{NE}, NaOH-EDTA-extractable iron; Ins6P, Inositol hexakisphosphate; NMR, nuclear magnetic resonance; OM, organic matter; P_i, inorganic P compounds; P_o, organic P compounds; sol-P, soluble P compounds; SOM, soil organic matter; P_{plant}, total P content in plant tissues; TP, total P content in soil.

* Corresponding author.
E-mail address: sara.martinengo@usys.ethz.ch (S. Martinengo).

https://doi.org/10.1016/j.geoderma.2025.117526
Received 2 July 2025; Received in revised form 29 August 2025; Accepted 28 September 2025

mononucleotides, and inositol phosphates, while the orthophosphate diesters include nucleic acids (DNA, RNA), phospholipids, and lipoteichoic acid. The phosphonate group, with a direct C-P bond, includes natural and manufactured compounds in soils, such as some antibiotics and the herbicide glyphosate (Cade-Menun and Liu, 2014; Cade-Menun, 2015).

Among soil constituents, iron (Fe) (hydr)oxides represent the most reactive surfaces with respect to the cycling of P compounds, particularly under fluctuating redox conditions such as those in paddy soils (Kögel-Knabner et al., 2010; Marschner, 2021). Indeed, rice is cultivated under flooded conditions for most of the cropping season, but soil aerobic conditions are periodically established during the season due to agronomic practices. Furthermore, rice roots are a well-known oxygen diffusion medium leading to the establishment of aerobic conditions, and the important implications of the redox gradient in rice rhizosphere over P availability have been recently pointed out (Martinengo et al. 2023; Martinengo et al., 2024). Notwithstanding the current knowledge in terms of P cycling under reducing conditions (Zhang et al. 2025), more careful evaluations are required to understand the effects of redox fluctuations during the rice growing cycle. Indeed, phosphate is strongly retained by redox-sensitive surfaces, but will be released when Fe (hydr) oxides experience reductive dissolution after soil flooding (Martinengo et al., 2023; Ponnamperuma, 1972; Scalenghe et al., 2002). This process has been widely linked to increased phosphate bioavailability in flooded soils (Wang et al., 2022a, b). Nevertheless, in a previous work we observed that the protraction of reducing conditions resulted in lower P uptake by rice plants (Martinengo et al. 2023). Consistent with the results of Zhang et al. (2003) and Santoro et al. (2019), we concluded that the released phosphate can be re-adsorbed or co-precipitated with aqueous Fe(II), thus decreasing the availability of the nutrient more than what was previously expected for flooded paddy soils. Similar to phosphate, many P_o compounds also may be retained during Fe(II) oxidative precipitation within the newly formed structures. This can occur through various mechanisms, including adsorption, precipitation and physical entrapment; the extent and kinetics of these mechanisms will depend on the specific P_o compound (Santoro et al., 2019; Wang et al., 2017). For example, phospholipids are retained during co-precipitation onto the coprecipitate surface only through weak physical interactions with limited protection, whereas inositol phosphates are rapidly and chemically adsorbed and/or precipitated, creating more stabilized, occluded coprecipitates (Celi et al., 2022; Santoro et al., 2019). Similarly to Fe-P_i co-precipitates, Fe-P_o co-precipitates also might be dissolved by the onset of reducing conditions (Kraal et al., 2019; Wang et al., 2017); however, the extent by which the mechanisms of P_o retention and/or release under reducing conditions might contribute to P availability in flooded paddy soils has been scarcely investigated.

Aside from abiotic stabilization processes, a further driver of P_o speciation in soil is represented by the activities of plants and soil microbes to acquire P from sparingly available pools. Recent investigations demonstrated that under P-limiting conditions the competition between rice roots and soil microbes can shift microbial P use toward the acquisition of P from organic sources by the hydrolysis of organic P compounds such as phospholipids, released from plant residues during decomposition (Wang et al., 2024). This means that the interplay between redox-driven co-precipitation and plant strategies to acquire P could on one hand increase the bioavailable P pool, but on the other hand cause a selective enrichment of specific P_o compounds in soil based on their affinity for the mineral phase (Celi et al., 2020; Prietzel et al., 2016; Santoro et al., 2023) and on the protection offered by these associations versus enzymatic hydrolysis (Giaveno et al., 2010, Giaveno et al., 2008). Considering that both plant and microbial activities for P acquisition are directly related to total soil P content (Richardson et al., 2009; Rose et al., 2013), the selective enrichment of P_o compounds can alter P speciation as a function of soil total P (TP) content. However, scant attention has been given to the effects of redox processes on P_o speciation and dynamics in paddy soils and their contribution to the P pool available for rice plants.

Based on these considerations we hypothesized that i) the quantity and forms of P_i and P_o compounds in paddy soils vary as a function of TP content; and ii) the composition of soil P_i and P_o species is driven by both redox-driven processes and the needs of rice plants. Thus, the objective of this study was to determine the speciation of P compounds and the mechanisms driving changes in speciation before and after rice cultivation, in a set of paddy soils differing in TP content.

2. Materials and methods

2.1. Experimental mesocosm setup and soil sampling

The soil samples analyzed in this study were collected from the mesocosm experiment described by Martinengo et al. (2023). Briefly, a set of 100 paddy topsoils was randomly collected from different sites to represent the rice cropping area of Lombardy (NW Italy) in the Po River plains. Most soils fell in the reference soil group of Luvisols and Cambisols, according to WRB classification (IUSS Working Group WRB, 2022). The GIS coordinates and detailed soil classification are reported in Martinengo et al. (2023). The soils were grouped according to their TP content into those with TP greater than 800 mg kg^{-1} (high-P soils), between 500 and 800 mg kg^{-1} (medium-P soils), and lower than 500 mg kg^{-1} (low-P soils). Within each group, two soils with pH higher than 6 and two soils with pH lower than 6 were selected and further characterized by a sand content below and above 50 % for each pH group. A total of 12 soils (Table 1) were thus chosen according to the grouping, and were used to grow rice (Martinengo et al., 2023).

Four mesocosms for each soil (biological replicates) were filled with 2.5 kg of fresh soil and then flooded by maintaining 5 cm of water above the soil surface. The Eh was measured potentiometrically to confirm the establishment of soil-reducing conditions (i.e., oxidation–reduction potential, ORP < -200 mV in all the soils). Seeds of the rice cultivar *Selenio* were pre-germinated for 3 days at 25 °C in the dark and transferred to the mesocosms after germination. Rice plants were then grown for 60 days under continuous flooding. Soils samples were collected before (*Pre*) and after (*Post*) rice growth. Samples were air-dried to mimic

Table 1
Physico-chemical properties of the twelve paddy soils selected in this study, including pH, sand content, total organic carbon (TOC), oxalate-extractable iron (Fe_{ox}), total phosphorus (TP), and 0.5 M $NaHCO_3$-extractable-P (Olsen P). Soils were divided into three groups based on their total P content; data are from Martinengo et al. (2023).

Soil ID	pH	Sand g kg^{-1}	Organic C g kg^{-1}	Fe_{ox} g kg^{-1}	TP mg kg^{-1}	Olsen P mg kg^{-1}
High-P						
HP a	6.1	770	13	1.47	893	60.1
HP b	5.8	250	20	6.53	899	59.7
HP c	5.7	780	9	0.62	877	39.3
HP d	5.9	570	10	4.70	810	50.4
High P mean ± std.dev	*5.9 ± 0.1*	*592 ± 214*	*13 ± 4*	*3.3 ± 2.39*	*869 ± 35.4*	*52.4 ± 5.07*
Medium-P						
MP a	6.4	840	10	0.74	549	21.8
MP b	6.9	420	10	3.34	512	15.9
MP c	7.9	290	10	3.41	541	40.2
MP d	6.6	620	6	0.53	534	15.8
Medium P mean ± std. dev	*6.9 ± 0.5*	*543 ± 208*	*9 ± 1.7*	*2.05 ± 1.37*	*534 ± 13.7*	*23.4 ± 2.37*
Low-P						
LP a	6.5	440	12	5.63	420	12.7
LP b	6.5	550	14	3.33	414	11.4
LP c	5.6	330	12	4.10	377	14.4
LP d	5.7	510	10	2.06	287	12.1
Low P mean ± std.dev	*6.1 ± 0.43*	*476 ± 83.5*	*12 ± 1.41*	*3.78 ± 1.29*	*374 ± 53.1*	*12.6 ± 1.02*

aerobic conditions occurring at the end of the rice growth cycle in the fields, sieved (<2 mm), and subjected to different analyses.

2.2. Soil P fractionation

Soil P pools were characterized in all 48 soil samples by sequential chemical fractionation as follows: a) soluble P [soluble-P; 0.1 M $CaCl_2$, 1 h reaction time for soluble P (Soltanpour et al., 1974)]; b) exchangeable P [exchange-P; anion exchange resins, 2 h contact time for desorbable P (Saggar et al., 1990)], representing the plant-available P pool; c) redox-sensitive P [Fe-P; acid ammonium oxalate, 2 h reaction time for P bound to amorphous Fe (hydro)oxides (Schwertmann, 1964)]. Although manganese (Mn) is also involved in redox reactions, the redox-sensitive P pool was entirely attributed to Fe, as Mn (hydr)oxides are mainly negatively charged in the pH range of the studied soils and do not contribute to P retention (Sposito, 2008). Residual P was calculated as the difference between TP determined by sulphuric-perchloric digestion and Fe-P. However, residual P may include both occluded P_i and P_o compounds not solubilized by the former extraction procedure (Olsen and Sommers, 1982), making it difficult to attribute residual P to P_i or P_o fractions. For this reason, residual P was not reported in the Results and Discussion sections.

In all extracts, molybdate-reactive phosphate (MRP) and molybdate-unreactive phosphate (MUP) were quantified. The MRP was determined colorimetrically (Murphy and Riley, 1962). Aliquots of the extracts were then dried at 105 °C, treated with concentrate sulphuric and perchloric acid and analyzed colorimetrically to determine the total extracted P content (Martin et al., 1999). Sulphuric and perchloric acid digestion may underestimate the P_o concentration in samples that contain inositol phosphate, due to incomplete digestion of this compound; for these soils, complete digestion was confirmed using *myo*-inositol hexakisphosphate (*myo*-Ins6P) as a standard. The MUP concentration was the difference between total extracted P and extract MRP concentrations. The MUP fraction includes mainly P_o along with some inorganic P forms that do not react with molybdate (Cade-Menun and Liu, 2014). For this study, we assumed that the MUP pool corresponded mainly to P_o forms. Therefore, we will hereafter refer to MRP and MUP in these extracts as P_i and P_o, respectively.

The values of P_i and P_o determined in each P pool before and after rice growth were used to calculate the percentage variation ($\Delta_{\%}$) in the specific pool, following the equation:

$$\Delta_{\%} = \frac{P_{Post} - P_{Pre}}{P_{Pre}} \times 100$$

where P_{Pre} and P_{Post} were the concentrations of P extracted in each P pool before and after rice growth, respectively.

The P_i and P_o concentrations obtained for each soil were averaged by soil P level, and the average concentratons for each soil P level were tested for statistically significant differences ($\alpha = 0.05$) by two-way ANOVA (i.e. soil P level and sampling time) followed by pair-wise post hoc analysis (Student-Newman-Keuls test). In a similar manner, the average values of $\Delta_{\%}$ for each P pool were tested for statistically significant differences ($\alpha = 0.05$) by one-way ANOVA (i.e., soil P level), followed by the same post hoc analysis. The statistical analyses were performed using the R version 4.1.1 (R Core Team, 2021). Normality and data homoscedasticity were checked with the Shapiro–Wilk and Levene tests, respectively. When necessary, data were transformed according to the data distribution by using the R function *box.cox* (R package "car").

2.3. Liquid-state ^{31}P NMR spectroscopy

Following the method of Cade-Menun and Preston (1996), 1 g of each soil (n = 48) was shaken overnight with 10 mL of 0.25 M NaOH and 50 mM EDTA (NaOH-EDTA). After centrifugation, the P_i and P_o concentrations in the extracts were determined as described above, using *myo*-Ins6P as a standard, and to test potential precipitation of humic-Fe complexes (Turner, 2008). The concentrations of Fe and Mn were determined by atomic absorption spectroscopy (AAS, PerkinElmer AAnalyst 400, Norwalk, CT, USA). The values of P_i, P_o, Fe and Mn obtained for each soil were averaged by soil P level, and the average values were tested for statistically significant differences ($\alpha = 0.05$) by two-way ANOVA (i.e. soil P level and sampling time) followed by pair-wise post hoc analysis as previously described.

The P_i and P_o concentrations in each extract were used to select one soil for each P level *Pre* and *Post* microcosm incubation (n = 6) to be analyzed by ^{31}P nuclear magnetic resonance spectroscopy (P-NMR). The solutions were freeze-dried and then resuspended in a 0.9 ml 1.0 M NaOH and 50 mM Na_2-EDTA solution and 0.1 ml deuterium oxide (Turner, 2008). Samples were analyzed on a JEOL ECZR 600 MHz instrument ($^1H\nu_{Larmor} = 600.23$ MHz; $^{31}P\ \nu_{Larmor} = 242.95$ MHz), using a 6 μs pulse (45°), a delay time of 2.0 s, an acquisition time of 0.4 s, and broadband proton decoupling (Turner, 2008). This delay time (2.4 s) was adequate for these soil extracts, based on the ratio of the concentrations of P to Fe plus Mn in each extract (Cade-Menun and Liu, 2014). Approximately 25,000 scans were acquired for each sample. Peak areas were calculated manually after integrating spectra processed with 7 Hz and 2 Hz line broadening using NUTS software (Acorn NMR, 2011 version). Methylene diphosphonic acid (MDPA) was added as a chemical shift reference. Peak identifications were made using a combination of visual inspection and automated peak picking and line fitting, and were assigned to P compounds based on the literature (Turner et al., 2012; Cade-Menun, 2015). Peak areas were converted to soil P concentrations (mg kg^{-1}) by multiplying the area of each peak by the total NaOH-EDTA P concentration for each sample. The results were corrected for orthophosphate diester degradation products by subtracting α- and β-glycerophosphate and the mononucleotides from the total orthophosphate monoester area and adding them to the total orthophosphate diester area (Chen et al., 2021).

2.4. Soil phosphatase activity

Potential phosphomoesterase activity was assayed at two pH ranges (Eivazi and Tabatabai. 1977) using air-dried soil samples, to give activities of alkaline phosphomonoesterase (Alk-PME) and acid phosphomonoesterase (Ac-PME). Although the determination on air-dried soil samples could significantly affect the absolute value of the enzymatic activity (Lane et al., 2022), this approach could be considered acceptable when treatment comparisons are the objective of the study and all samples have been subjected to the same storage conditions (Peoples and Koide, 2012). In brief, Alk-PME and Ac-PME were assayed with a modified universal buffer at pH 11.0 and 6.5, respectively, using *p*-nitrophenyl phosphate (*p*NP) as substrate for the enzymatic reaction. The released *p*-nitrophenol (*p*N) was measured spectrophotometrically at 400 nm and the activities were expressed as mg *p*N kg^{-1} dry soil h^{-1}. The specific enzymatic activity is generally calculated as the ratio between enzyme activity and soil total organic C or microbial C content (Raiesi and Beheshti, 2014; Trasar-Cepeda et al., 2008). However, considering that P_o compounds are the target substrates for Ac-PME and Alk-PME, and plant and/or microbial enzymatic activity has been related to the soil P content (Rose et al., 2013; Wang et al., 2024), for this study, the specific enzymatic activity was calculated as the ratio between Ac-PME and Alk-PME activity and the values of soil total P_o, considering that inositol phosphatases (i.e., phytases) can act on *p*NP-phosphate substrate (Zhu et al., 2013). The values of Ac-PME and Alk-PME obtained for each soil were averaged by soil P level, and the average values for each enzyme were tested for statistically significant differences ($p < 0.050$) by two-way ANOVA (i.e. soil P level and sampling time) as previously described.

3. Results

3.1. Soil P fractions

Fig. 1 shows the distribution of P_i and P_o concentrations in the operationally-defined P pools and their variations with rice growth. Statistically significant variations in P_i concentrations were observed for the interaction between soil P level and sampling time ($p < 0.05$). In all cases, the predominant P_i pool was Fe-P_i, followed by exchange-$P_i \gg$ soluble-P_i. Although the soluble-P_i concentrations were significantly lower than the other P_i pools, a variable amount of soluble-P_i was measured in all soils (high-P = 4.50 mg kg^{-1}, medium-P = 0.59 mg kg^{-1}, low-P = 0.32 mg kg^{-1}). In almost all P_i pools the highest concentrations were observed for the high-P soil group and in the soils collected before rice growth, albeit some differences were observed according to soil P level. In particular, in medium-P and low-P soils concentrations of Fe-P_i were higher after 60 days of rice growth compared to soils before rice growth. The percentage variation of P_i in each operationally-defined pool was statistically affected by the interaction between soil P level and sampling time ($p < 0.01$, Fig. 1). The greatest variations were observed for soluble-P_i and exchange-P_i pools, particularly in high-P soils, where both pools were more than halved after rice growth. Conversely, rice growth resulted in a slight increase in soluble-P_i and only a small modification of exchange-P_i in medium-P and low-P soils. This trend was also observed for Fe-P_i and was particularly marked in low-P soils where the Fe-P_i doubled after rice cultivation.

Organic P concentrations were generally lower than P_i concentrations, but also in this case the highest concentrations for most P_o pools were observed in high-P soils, while smaller differences were found in medium-P and low-P soils (Fig. 1). In all cases, the predominant P_o pool was Fe-P_o, followed by exchange-P_o, and soluble-P_o, albeit the differences among soil P_o pools were less pronounced compared to those presented for P_i. The percentage variation of each P_o pool during rice growth mostly resembled the variation of P_i pools (Fig. 1), albeit with more pronounced differences for soluble-P_o and exchange-P_o. The former showed an opposite trend compared to what described for soluble-P_i, as in this case the greatest depletions were measured in medium-P and low-P soils respectively. Exchangeable-P_o generally decreased in all soil groups, while Fe-P_o showed a slight increase in high-P soils and a sharp decrease in medium- and low-P soils.

3.2. Phosphorus forms identified by ^{31}P NMR spectroscopy

There was a significant ($p < 0.05$) interaction of soil P level and sampling time for the concentrations of NaOH-EDTA extractable-P_i when all soils were extracted (Table 2). The highest NaOH-EDTA P_i concentrations were measured in high-P soils before rice growth followed by *Post* high-P and medium-P, as well as *Pre* medium-P soils. The low-P soils had the lowest P_i concentrations in the NaOH-EDTA extracts, with no significant differences with sampling time. The NaOH-EDTA extractable-P_o concentrations were not significantly different with soil P level or sampling time, and averaged 42.0 mg kg^{-1}, which was less than 10 % of the soil TP (Table 2). The NaOH-EDTA-extractable Fe (Fe_{NE}) concentrations did not show a significant interaction of P level*time; in soils with different P levels (averaging dates together for each P level), high-P soils had significantly ($p < 0.05$) greater Fe_{NE} (122 mg

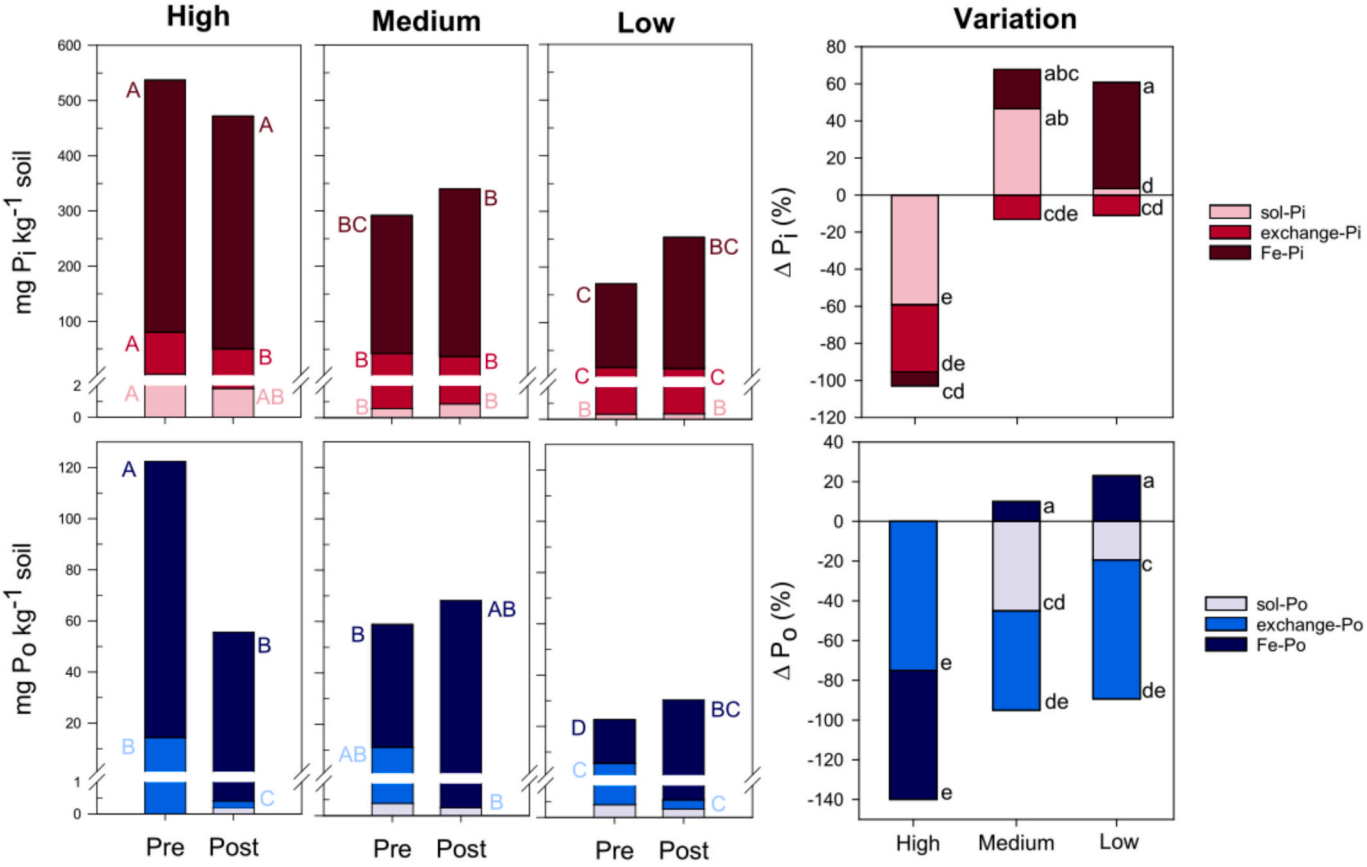

Fig. 1. Distribution of inorganic P (P_i) and organic P (P_o) concentrations in the operationally-defined pools determined during sequential fractionation [sol-P (0.1 M $CaCl_2$), exchange-P (anion exchange resins), and Fe-P (acid ammonium oxalate)] and their percentage variation in high-P, medium-P and low-P soils before (Pre) and after (Post) 60 days of rice growth under continuously flooded conditions. Upper-case letters represent statistically significant differences for the interaction P level*sampling time in the same P pool (p-value < 0.05), smaller-case letters represent statistically significant differences for the interaction soil P level*P pool (p-value < 0.01). For the sake of graph readability, error bars were not included in the figures.

Table 2
Mean concentrations (and relative standard errors) of inorganic P (P_i) and organic P (P_o) in the 0.25 M NaOH – 50 mM EDTA extracts of the twelve soils before (Pre) and after (Post) 60 days of rice growth under continuous flooding. Values in the table represent the average of four independent replicates for each of the four soil in the same P level designated as high-P, medium-P and low-P soils prior to the start of the experiment (n = 16).

Soil P level	Time	TP		P_i[a]		P_o[b]	
		mg kg^{-1}	(% TP)	mg kg^{-1}	(% TP)	mg kg^{-1}	(% TP)
High-P	*Pre*	518 ± 59.0	59 ± 6.5	477 ± 40.2a	65 ± 4.5	41.6 ± 8.5	4.7 ± 0.9
	Post	411 ± 80.0	57 ± 8.2	342 ± 46.1b	61 ± 5.2	69.6 ± 7.2	8.0 ± 0.7
Medium-P	*Pre*	318 ± 11.7	56 ± 2.6	276 ± 20.9c	51 ± 4.9	41.4 ± 2.3	7.8 ± 0.3
	Post	377 ± 10.3	41 ± 2.5	345 ± 21.4b	64 ± 5.0	32.0 ± 1.8	6.0 ± 0.3
Low-P	*Pre*	160 ± 10.5	55 ± 2.2	127 ± 6.12d	46 ± 1.3	33.5 ± 4.1	8.6 ± 0.7
	Post	160 ± 16.1	55 ± 1.7	126 ± 5.83 d	46 ± 1.1	33.8 ± 6.6	9.0 ± 1.1
p-value Soil P level				*< 0.01*		*n.s*	
p-value Sampling time				*n.s*		*n.s*	
*p-value P level*time*				*< 0.05*		*n.s*	

[a] Determined colorimetrically (molybdate-reactive P).
[b] Determined as the difference between colorimetric P concentration after digestion and P_i (molybdate-unreactive P).

kg^{-1}), than both medium-P (67.3 mg kg^{-1}) and low-P (71.3 mg kg^{-1}) soils, which were not significantly different from each other. And overall (averaging all P levels together), Fe_{NE} concentrations were significantly greater in *Post* soils (97.0 mg kg^{-1}) than *Pre* soils (77.0 mg kg^{-1}; $p < 0.01$). Concentrations of Mn in NaOH-EDTA extracts were not significantly different with time or among soil P groups, resulting in an average Mn concentration of 49.4 mg kg^{-1}.

The NaOH-EDTA-extractable P concentrations of the soils selected for ^{31}P-NMR (Table 3) were generally within the averages for the entire soil set (Table 2). Extraction with NaOH-EDTA recovered 42–74 % of soil TP, with a greater percentage of TP extracted from high-P soils (74 %), compared to medium-P (45 %) and low-P (42 %) soils. In the ^{31}P-NMR spectra, the chemical shifts for orthophosphate and MDPA were 6.00 ± 0.00 ppm and 17.26 ± 0.00 ppm, respectively (Figs. 2A, 2B). Orthophosphate represented 55.6–85.1 % of extracted P, and orthophosphate concentrations were highest in the high-P samples (Table 3). Other detected P_i compounds were pyrophosphate (−4.25 ppm) and various polyphosphate peaks (e.g., −4.25, −5.89, −7.60, −9.76, and −10.41 ppm), with no clear differences among soils for the presence of peaks in this region. Note that these and other chemical shifts reported for this study are means of chemical shifts of peaks in at least four of the six soil samples; the standard deviations of these means are ± 0.05 ppm or less and so will not be reported. For these samples, the polyphosphate region was from −4.25 to −12 ppm, rather than to −25 ppm as is often used. However, there was no evidence of signal aliasing to suggest that a larger spectral window should have been used for these samples, and peaks in this region were less than 5 mg kg^{-1} extracted P for all samples.

Organic P compound classes in spectra were grouped into phosphonates (21.0 to 7.5 ppm), orthophosphate monoesters (7.5 to 6.1 ppm and 2.9 to 2.4 ppm), and orthophosphate diesters (2.5 to −4 ppm; Fig. 2). Total organic P determined from the ^{31}P-NMR spectra was 43.3 to 13.9 % of extracted P (Table 3), which is higher than was determined by digestion and colorimetry (Table 2). Peaks for unidentified phosphonate compounds were detected at 25.88, 23.81, 22.16, 21.28, 19.37, 17.55, 17.07, 16.83, 16.24, and 10.25 ppm, with no clear trends among

Table 3
Phosphorus compounds determined by NaOH-EDTA extraction and solution ^{31}P NMR spectroscopy in the high-P, medium-P and low P-soils, before (Pre) and after (Post) 60 days of rice cultivation under continuous flooding conditions. Values are mg P kg^{-1} soil (percentage extracted P), with the exception of NaOH-EDTA P, for which values are mg P kg^{-1} soil (percentage soil total P (TP)).

	High-P		Medium-P		Low-P	
	Pre	*Post*	*Pre*	*Post*	*Pre*	*Post*
NaOH-EDTA P (% TP)	606 (67)	665 (74)	216 (42)	232 (45)	158 (42)	174 (46)
Inorganic P compounds	*435.7 (71.9)*	*484.1 (72.8)*	*142.6 (66.0)*	*177.5 (76.5)*	*89.6 (56.7)*	*149.8 (86.1)*
Orthophosphate	431.5 (71.2)	479.5 (72.1)	139.1 (64.4)	175.6 (75.7)	88.3 (55.9)	148.2 (85.2)
Pyro+polyphosphates[a]	4.2 (0.7)	4.7 (0.7)	3.5 (1.6)	1.9 (0.8)	1.3 (0.8)	1.6 (0.9)
Organic P compounds[b]	*170.3 (28.1)*	*180.9 (27.2)*	*73.4 (34.0)*	*54.5 (23.5)*	*68.4 (43.3)*	*24.2 (13.9)*
Phosphonates	22.4 (3.7)	24.6 (3.7)	8.4 (3.9)	5.6 (2.4)	4.0 (2.5)	4.5 (2.6)
Orthophosphate monoesters[c]	*117.0 (19.3)*	*121.0 (18.2)*	*29.8 (13.8)*	*35.7 (15.4)*	*25.0 (15.8)*	*11.7 (6.7)*
myo-Ins6P	23.6 (3.9)	18.0 (2.7)	6.0 (2.8)	4.6 (2.0)	3.3 (2.1)	2.4 (1.4)
scyllo-Ins6P	12.1 (2.0)	14.0 (2.1)	3.0 (1.4)	3.0 (1.3)	1.1 (0.7)	1.2 (0.7)
chiro-Ins6P	10.3 (1.7)	9.3 (1.4)	1.5 (0.7)	3.0 (1.3)	2.2 (1.4)	1.2 (0.7)
neo-Ins6P	10.3 (1.7)	4.7 (0.7)	1.5 (0.7)	4.6 (2.0)	2.2 (1.4)	1.2 (0.7)
Total Ins6P	*37.0 (9.3)*	*32.6 (6.9)*	*15.1 (5.6)*	*12.3 (6.6)*	*17.5 (5.6)*	*4.9 (3.5)*
Choline phosphate	4.2 (0.7)	4.7 (0.7)	0.6 (0.3)	1.6 (0.7)	0.5 (0.3)	0.5 (0.3)
Glucose 6-phosphate	1.8 (0.3)	2.0 (0.3)	1.5 (0.7)	1.6 (0.7)	1.1 (0.7)	0.5 (0.3)
Monoester 1	7.9 (1.3)	4.7 (0.7)	2.2 (1.0)	3.0 (1.3)	1.6 (1.0)	1.2 (0.3)
Monoester 2	27.3 (4.5)	41.2 (6.2)	10.4 (4.8)	12.5 (5.4)	10.7 (6.8)	2.1 (1.2)
Monoester 3	19.4 (3.2)	22.6 (3.4)	3.0 (1.4)	1.6 (0.7)	2.2 (1.4)	1.2 (0.7)
Orthophosphate diesters[c]	*30.9 (5.1)*	*35.2 (5.3)*	*26.8 (16.3)*	*13.2 (5.7)*	*28.0 (25.0)*	*7.3 (4.6)*
DNA	0.0 (0.0)	0.0 (0.0)	0.4 (0.2)	0.5 (0.2)	0.2 (0.1)	0.7 (0.4)
Other diester 1	6.7 (1.1)	6.7 (1.0)	4.1 (1.9)	2.6 (1.1)	0.9 (0.6)	2.1 (1.2)
Other diester 2	2.4 (0.4)	3.3 (0.5)	0.6 (0.3)	0.7 (0.3)	0.2 (0.1)	0.3 (0.2)
α-glycerophosphate[c]	4.2 (0.7)	4.7 (0.7)	9.1 (4.2)	1.6 (0.7)	12.0 (7.6)	1.2 (0.7)
β-glycerophosphate[c]	8.5 (1.4)	9.3 (1.4)	17.9 (8.3)	3.2 (1.4)	24.0 (15.2)	2.4 (1.4)
Mononucleotides[c]	9.1 (1.5)	11.3 (1.7)	3.0 (1.4)	4.6 (2.0)	2.2 (1.4)	1.2 (0.7)
Monoester:Diester[d]	3.78	3.43	1.11	2.7	0.89	1.60

[a] Sum of pyrophosphate and polyphosphate peaks.
[b] Sum of orthophosphate monoesters and diesters.
[c] Values corrected for diester degradation products by subtracting α- and β-glycerophosphate and the mononucleotides from the total monoester area and adding them to the total diester area.
[d] Ratio of orthophosphate monoesters to orthophosphate diesters (corrected for degradation).

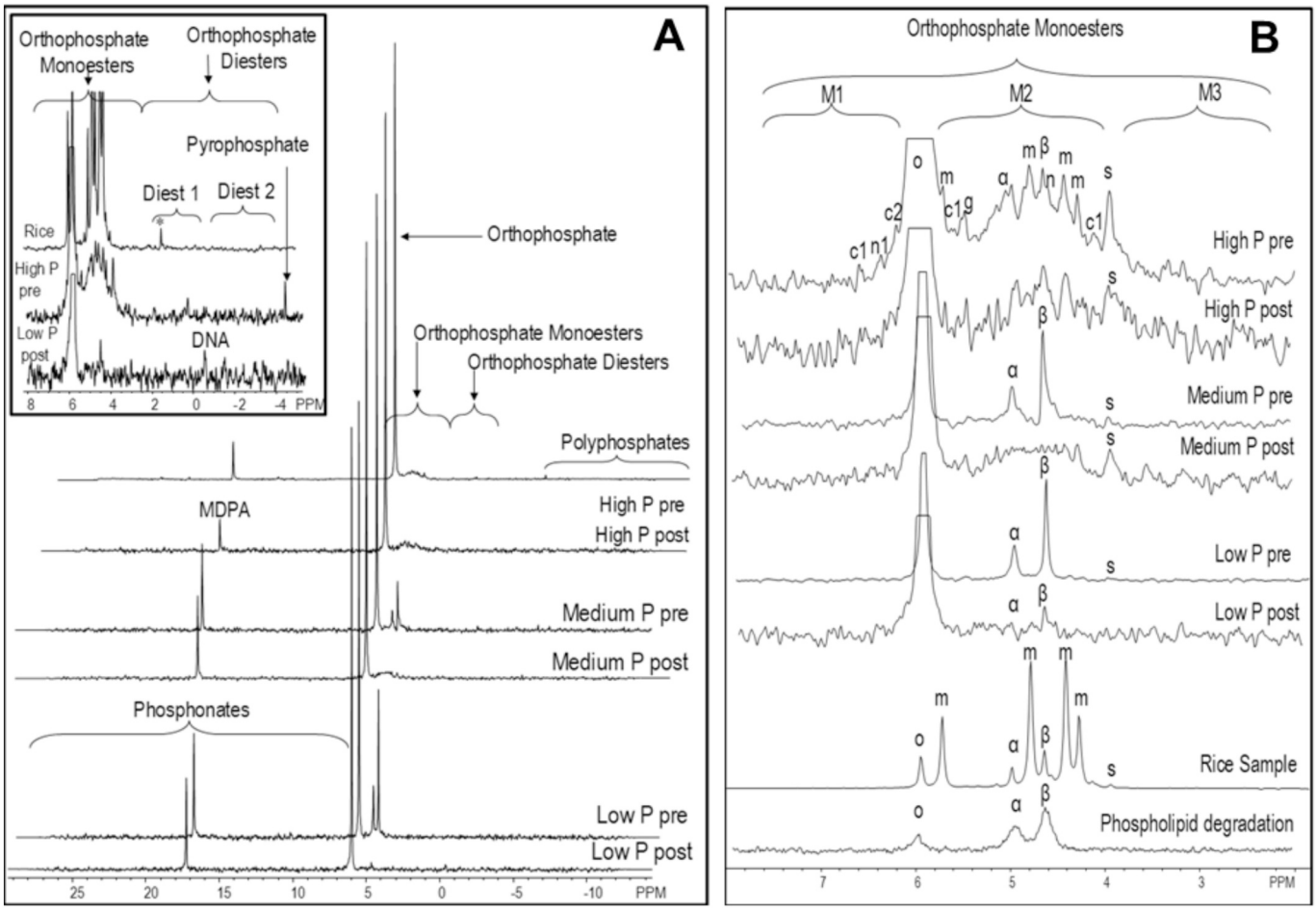

Fig. 2. Solution ^{31}P-NMR spectra of NaOH-EDTA extracts from high-P, medium-P, and low-P soils before (Pre) and after (Post) 60 days of rice growth. A. The main figure shows full spectra for each soil sample, all scaled to the height of the orthophosphate peak. The inset shows details of the region from 8 to −5 pm for two soil samples. B. Spectra for all soil samples, showing details of the region from 8 to −2 ppm, plus the spectrum a rice plant sample analyzed with the soil samples for this study and a spectrum showing degradation of the phospholipid L-α-phosphatidyl choline (analyzed for Cade-Menun, 2015). All spectra shown processed with 7 Hz line-broadening. Not all peaks are labeled in each spectrum. See text for more details about regions and peaks. Diest1, Diest2: orthophosphate diester regions; M1, M2, M3: orthophosphate monoester regions; MDPA, methylene diphosphonic acid; c1, c2: D-*chiro*-inositol hexaphosphate (Ins6P); m, *myo*-Ins6P; n, *neo*-Ins6P; o, orthophosphate; s, *scyllo*-Ins6P; α, β: α- and β-glycerophosphates. The * indicates an unidentified peak in orthophosphate diester region of the rice sample in the inset.

soils. The majority of these peaks were also detected in rice grain samples analyzed at the same time. Phosphonates represented < 5 % of extracted P for all samples.

Compounds in the orthophosphate monoester region (after correcting for degradation) were 9.9–103.1 mg kg^{-1} (6.7–19.3 % extracted P), with highest concentrations, and highest proportion of total extracted P, in the high-P soil samples. Peaks for four Ins6P stereoisomers were identified in all samples: *myo*-Ins6P at 5.84, 4.82, 4.49 and 4.35 ppm and *scyllo*-Ins6P at 3.97 ppm in all samples; D-*chiro*-Ins6P in the 4 equatorial/2 axial conformer at 6.67, 5.57 and 4.21 ppm and in the 2 equatorial /4 axial conformer at 6.26, 5.01 and 4.62 ppm in all samples; *neo*-Ins6P in the 4 equatorial/2 axial conformer at 6.46 and 4.66 ppm in all samples, and *neo*-Ins6P in the 2 equatorial/4 axial conformer at 4.87 and 5.10 ppm for all but the high-P *Post* sample. Peaks for choline phosphate and glycerophosphate were identified at 4.09 and 5.51 ppm, respectively in all samples. The remaining unidentified orthophosphate monoester peaks were divided into three regions (Fig. 2B): the Monoester 1 region had peaks at 7.37, 6.98, and 6.16 ppm in most samples; the Monoester 2 region had peaks at 5.64, 5.17 and 4.76 ppm in all samples and would also include the underlying broad peak, which was minimal in these samples; and the Monoester 3 region had peaks at 3.77, 3.57 and 3.12 ppm in all samples. Of the orthophosphate monoesters in these samples, the total Ins6P stereoisomers represented the highest P concentrations and greatest proportion of extracted P. Peaks for the *myo*- and *scyllo*-Ins6P stereoisomers were confirmed by comparison with those in the spectrum of rice grain samples (Fig. 2B).

Peaks in the orthophosphate monoester region in the P-NMR spectra were divided into DNA, and the Other diester1 and Other diester2 groups (Fig. 2A inset). Peaks for DNA were found at −0.66 and −0.75 ppm for medium-P and low-P *Pre* and *Post* samples, but were not present in either of the high-P samples. Peaks in the Other diester1 region were detected at 2.43 ppm, 2.09 ppm, 1.81 ppm, 1.59 ppm, 1.20 ppm, 0.9 ppm, and 0.55 ppm. Most of these peaks are for lipoteichoic acids and phospholipids, and were also detected in rice plant samples (in the Fig. 2A inset, a prominent peak in this region is indicated with *). Peaks in the Other diester2 region were detected at −1.39, −1.75, −2.84, −3.28 and −3.74 ppm, but the compounds with peaks in this region are unknown. Peaks for mononucleotides were detected in all samples at 4.42, 4.38 and 4.34 ppm, as were peaks for α- and β-glycerophosphates at 5.04 and 4.68 ppm, respectively. However, while these appear in the orthophosphate monoester region in spectra, they originate from the degradation of compounds that were orthophosphate diesters in the original soils prior to extraction with NaOH-EDTA and analysis by ^{31}P NMR; α- and β-glycerophosphates from phospholipids, and mononucleotides from RNA (Cade-Menun and Liu, 2014; Chen et al. 2021), with α- and β-glycerophosphate in the classic 1:2 proportion typical of

phospholipid degradation (Fig. 2B). While present in all samples, combined these peaks were 12.5 and 22.8 % of extracted P in the medium-P and low-P *Pre* samples, dropping to 2.1 % of extracted P in the medium-P and low-P samples post-incubation, the same proportion for the high-P *Pre* and *Post* samples (Table 3). These compounds were also present in the rice grain samples, although at a lower proportion of extracted P (Fig. 2B). When corrected for these degradation compounds, the Monoester:Diester ratios (Table 2) show that orthophosphate monoesters are the dominant compound class for high-P samples at both sampling dates and *Post* incubation for medium-P and low-P soils, but orthophosphate diesters are more abundant prior to incubation for the medium-P and low-P soils.

3.3. Enzymatic activity

Enzymatic activities were measured in all soils before and after rice growth. The potential activities of Ac-PME were much higher than those of Alk-PME for all soils, and only the former were significantly influenced by time. Aside from the more favorable soil pH (Eivazi and Tabatabai 1977; Wu et al. 2021), which ranged between 5.9–6.9, acid phosphatases are produced by plant roots and soil microbes, while alkaline phosphatases are produced only by free-living microorganisms (Hofmann et al., 2016). In general, in all studied soils, acid phosphatase activity was much higher than alkaline phosphatase and increased with rice growth.

The Ac-PME activities measured in *Post* rice growth soils were significantly higher than those measured in *Pre* soils (Fig. 3a). The opposite was true for Alk-PME activities, which resulted in slightly higher values before rice cultivation, albeit the differences were not statistically significant. Specific enzymatic activities showed greater differences among soils (Fig. 3b), although only specific Ac-PME activities showed a significant interaction of P level and sampling time ($p < 0.05$). Indeed, specific enzyme activities were significantly higher in low-P and medium-P soils after rice growth compared to before rice growth and compared to high-P soils before and after rice growth.

4. Discussion

In this study, we hypothetized that soil TP content influences abiotic and biotic processes controlling the distribution of P_i and P_o forms. Consistent with this hypothesis, the distribution of operationally-defined P forms across wet chemical extractions discussed in Section 3.1 (Fig. 1) showed that P concentration was low in all soils in the soluble and exchangeable P_i pools, with only small differences among the three soil P groups. In contrast, the redox-sensitive P_i pools represented on average 17 % of TP with a clear differentiation among the three soil P groups. Computation of the percentage variation before and after rice growth (Fig. 1) showed a decrease in the exchangeable P_i pool while the soluble P_i pool was depleted only in high-P soils and remained quite constant in the other soils. Considering that the exchangeable-P_i pool represents the amount of P that is displaced from the soil surfaces after the consumption of soluble P_i (Moody et al., 2013), the apparently static behavior of soluble-P_i during rice growth can be explained by P in the exchangeable-P pool replacing the P taken up by rice plants from the soluble-P pool, consistently with the strong positive correlation we previously observed between soil exchangeable-P and plant P uptake

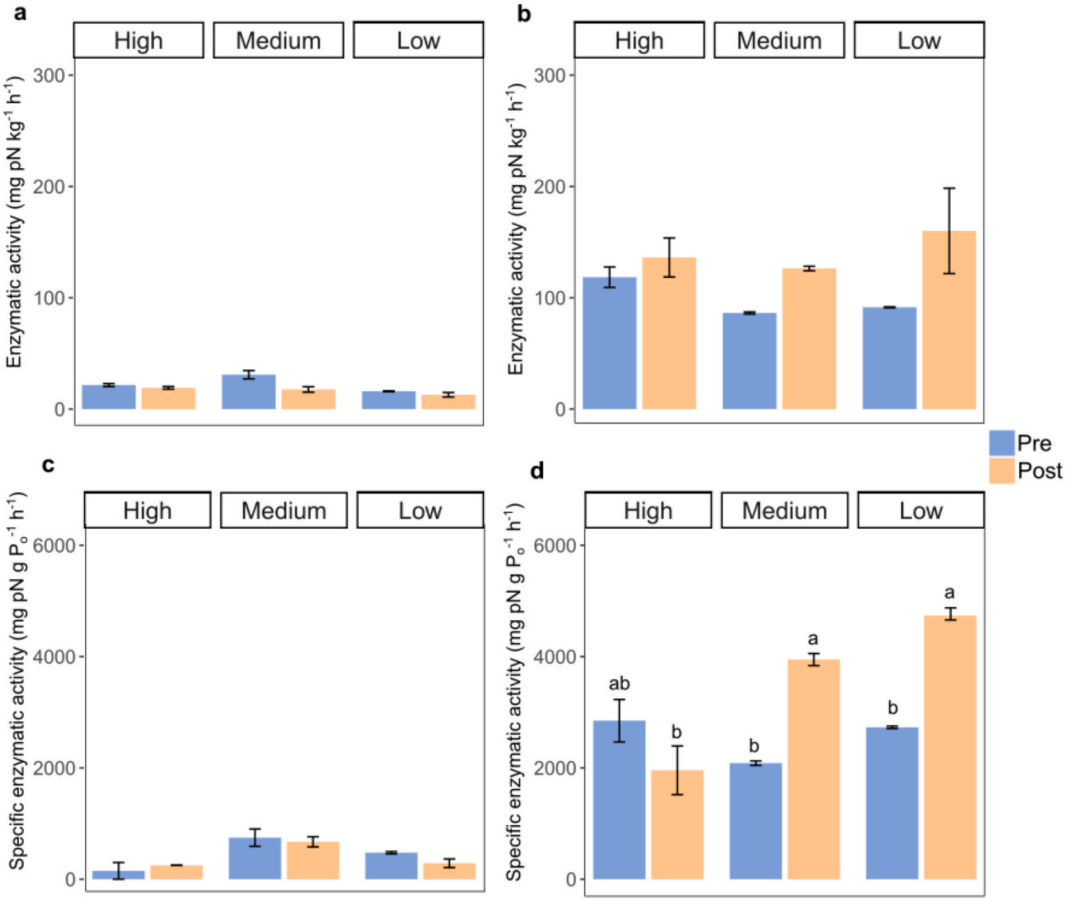

Fig. 3. Activities of a) alkaline phosphatase, b) acid phosphatase, and specific enzymatic activity normalized to the values of soil total P_o of c) alkaline phosphatase and d) acid phosphatase in the high-P, medium-P and low-P soils before (Pre) and after (Post) 60 days of rice growth. Each value represents the average among four independent replicates, bars represent the standard errors. Different letters indicate statistically significant differences for the interaction P level*time (p-value < 0.05).

(Martinengo et al., 2023). However, the exchangeable-P pool also appeared to feed the redox-sensitive P_i pool, which increased in medium-P and low-P soils after rice growth. Although the soils under reducing conditions experienced reductive dissolution of Fe (hydr)oxides with an expected increase of P in the soil solution (Scalenghe et al., 2002; Wang et al., 2022a; Zhang et al., 2025), co-precipitation processes may occur during soil flooding (Martinengo et al., 2023; Santoro et al., 2019; Zhang et al., 2003), especially when the reducing conditions are protracted (Heiberg et al., 2010; Refait et al., 2007). This may explain the generally high content of redox-sensitive P measured in paddy soils (Darilek et al., 2010). It is therefore likely that the P_i promptly released by reductive dissolution in the first 7–14 days after soil flooding was subsequently co-precipitated with the aqueous Fe(II), thus feeding the redox-sensitive P pool. This behavior was observed also in open fields in temperate regions (NW, Italy) during the first 60–70 days of the crop season, followed by a subsequent decrease of the redox-sensitive P fraction after plant tillering (Lizcano Toledo et al., 2022), due to the increasing needs of P by the growing plants. Martinengo et al. (2023) concluded that the P associated with reductively dissolvable Fe (hydr) oxides could not be the only nor the most relevant P pool for plants, probably because of an observed asynchrony between P_i release into soil solution and plant requirements. Additionally, in moderately weathered soils, the crystallization of Fe minerals is less pronounced than in highly weathered subtropical environments (Huang et al., 2016), likely making them more sensitive to redox-temporal variations and altering their role as source or sink of P for plants during the rice growth as a function of soil P content (Martinengo et al. 2023).

Soil P_o pools presented similar dynamics, although variations in operationally-defined pools from wet chemical extractions were less pronounced (Section 3.1, Fig. 1). The negative variation of exchangeable P_o and redox-sensitive P_o with rice growth in high P-soils (Fig. 1) may be related to the high availability of P_i for plant uptake. In contrast, in medium-P and low-P soils the negative variations of soluble and exchangeable P_o were accompanied by a positive variation of the redox-sensitive P_o pool (Fig. 1), confirming that P_o forms are strongly affected by Fe reduction and oxidation processes. Although P_o forms are governed by abiotic reactions, they also undergo more complex biotic processes than P_i compounds.

The differences we observed in the variation of operationally-defined P_i and P_o pools can be attributed to the complexity of soil P speciation. While P_i pools are primarily composed of phosphate, the P_o pools contain a wide range of compounds encompassing several chemical compound classes (Cade-Menun, 2005; Turner et al., 2005; Cade-Menun, 2015). Each of these compounds exhibited different behaviors during Fe(III) reductive dissolution and subsequent Fe(II) oxidative precipitation (Santoro et al. 2019; Wang et al. 2017), potentially impacting the alternating Fe-P coprecipitation/dissolution processes. This, in turn, affects the distribution of compounds in P_o pools and their potential as phosphate sources for plant nutrition.

Consistently, the ^{31}P NMR spectra before rice cultivation clearly show net differences in P_o composition as a function of total soil P content (Tables 2, 3; Fig. 2b). High-P soils were characterized by the prevalence of orthophosphate monoesters, including *myo*-, *scyllo*-, *chiro*- and *neo*-inositol phosphates and a lower contribution of orthophosphate diesters (Table 3). Their presence may be related to the contribution of rice leaves and roots, which, however, contain relatively greater amounts of orthophosphate diesters than monoesters (Duersch et al., 2020). It can be inferred that, once plant residues have been incorporated in soil, inositol phosphates may progressively and selectively accumulate through the repeated redox cycles occurring during the decades of monocultural rice cropping characterizing the soils from NW Italy Po plain (Miniotti et al., 2016; Sodano et al., 2017; Zampieri et al., 2019). This could be due to the well-known greater affinity of inositol phosphates for Fe (hydr)oxides with respect to orthophosphate diesters, such as phospholipids and nucleic acids residues (Celi and Barberis, 2005). In rice soils, the selective enrichment of inositol phosphates could be, on one hand, emphasized by co-precipitation processes occurring during oxic periods that retain more P than sorption (Chen et al., 2024; Santoro et al., 2019; Senn et al., 2015); on the other hand, it could be decreased with the establishment of anaerobic conditions, due to Fe (hydr)oxide reductive dissolution and the release of associated P forms. Consequently, in rice soils, the extent to which inositol phosphates can be selectively accumulated over other organic compounds may be lower than what is generally observed under aerobic conditions (Recena et al., 2018).

After rice growth, the NaOH-EDTA-extracted P_o from the high-P soils was slightly enriched in mononucleotides and α-glycerophosphates (Table 3), which together with a lower decrease of *myo*- and *neo*-inositol phosphates, contributed to maintaining nearly unchanged the level of P_o (Table 2). As the amount of NaOH-EDTA-extracted P_o is comparable to the sum of soluble-P_o + exchange-P_o + Fe-P_o, we can assume that the reducing conditions established during rice growth may have caused a consistent release into the soil solution of P_o forms associated with Fe (hydr)oxides. In addition, the active rhizosphere could have enriched the surrounding environment with plant- or microbial-derived orthophosphate diesters (De Sena et al., 2022). This was also accompanied by the pronounced signals of *scyllo*-inositol phosphates, which confirm an active microbial community (Liu et al., 2018). These compounds accumulated in the high-P soils (Fig. 2b) and compensated the P_o losses due to mineralization processes, maintaining nearly unchanged the net P_o pool, as also supported by the lack of differences in the specific enzymatic activity of Ac-PME before and after rice growth. In high-P soils, the legacy P pool was largely sufficient to guarantee a high P availability and feed both rice roots and soil microbial communities (Wang et al., 2024), without requiring an increase in enzymatic activity to release phosphate from P_o compounds. Indeed, notwithstanding the greater P_o pool present in high-P soils, the enzymatic activity was not statistically different from the soils with lower P_o and did not change during rice growth, when the reducing conditions may further increase the P_o compounds that can undergo enzymatic hydrolysis. Thus, we can infer that both biotic and abiotic processes affected the soil P_o composition, although abiotic stabilization seemed to dominate, changing the proportion between orthophosphate monoesters and diesters.

In contrast, medium-P and low-P soils, before rice growth, presented a different P_o speciation with comparable amounts of orthophosphate monoesters and diesters. Spectra were dominated by α- and β-glycerophosphates; the 1:2 ratio of α- to β-glycerophosphate is typical of the hydrolysis of phospholipids during NMR extraction and analysis, caused by the high pH NaOH-EDTA extractant (Doolette et al., 2009; Cade-Menun and Liu, 2014; Colocho Hurtarte et al., 2020). The presence of these labile compounds could be related to a larger contribution of fresh/unaltered plant material (Duersch et al., 2020) and microbially synthesized compounds (Wu et al., 2021) to the whole P_o pool, while inositol phosphates represent a lower fraction.

With rice growth, the soils with lower P content experienced a net depletion of P_o, with drastic losses of α- and β-glycerophosphates, and mononucleotides in the low-P soils (Table 3; Fig. 2b). This suggests an active utilization of the more labile P_o pool (De Sena et al. 2022), hydrolyzed by phosphodiesterases and phosphomonoesterases (Wu et al. 2021). Under the same experimental conditions, Martinengo et al. (2023) highlighted that the low P availability led to the activation of plant strategies to overcome P limitation, further exacerbating the competition between rice roots and soil microorganisms for both C and P (Wang et al. 2022b). As recently demonstrated by Wang et al. (2024), this competition makes the mining from additional P sources necessary, thus increasing the specific enzymatic activity of Ac-PME to acquire phosphate from P_o compounds present in the fresh/undecomposed plant residues. Indeed, the low amount of available P may stimulate microorganisms to produce PME (Peng et al., 2021; Wu et al., 2021) but also other hydrolytic enzymes that catalyze organic matter decomposition and contribute to phosphate release.

5. Conclusions

With this study, we demonstrated the fundamental interconnection between total soil P content and the dynamics of inorganic and organic P pools, ultimately presenting new insight into the role of soil P speciation in regulating nutrient availability under flooding conditions typical of rice cultivation. In high-P soils, P availability for rice is sustained by P_i present in the soil solution, continuously fed by less-labile P_i pools, while P_o speciation reflects long-term redox cycling, leading to the selective accumulation of phosphate monoesters like inositol phosphates. Conversely, soils with limited P content rely on a rapid turnover of α- and β-glycerophosphates from phospholipids and mono-nucleotides—labile P_o compounds that cycle quickly and release phosphate to support plant uptake.

These findings suggest that soil P legacy and redox-driven transformations can be strategically leveraged to optimize P use efficiency in rice systems. Tailored water management practices that modulate redox conditions, together with a deeper understanding of microbial community interactions with P_o forms, may enhance the mobilization of legacy P in low-P soils and reduce dependence on external P inputs.

Future research should explore the biotic–abiotic feedback that govern P_o transformations under dynamic redox regimes. This knowledge could inform the development of precision soil management strategies that support both agronomic productivity and long-term sustainability of rice agroecosystems.

6. Statements & declarations

Research carried out in the framework of the P-RICE research project “ Fosforo in risaia: equilibrio tra produttività e ambiente nell’ottica delle nuove pratiche agronomiche ” selected with the call for funding of research projects in agriculture and forestry 2018 of Regione Lombardia. Project funded with d.d.s. March 28th – n. 4403. The authors have no competing interests to declare that are relevant to the content of this article.

CRediT authorship contribution statement

Sara Martinengo: Writing – review & editing, Writing – original draft, Methodology, Formal analysis, Data curation, Conceptualization. **Lia Chilà:** Formal analysis. **Martina Mazzon:** Writing – review & editing, Formal analysis. **Barbara Cade-Menun:** Writing – review & editing, Methodology, Formal analysis, Data curation, Conceptualization. **Simone Bordignon:** Writing – review & editing, Methodology, Formal analysis, Data curation. **Roberto Gobetto:** Writing – review & editing, Methodology, Conceptualization. **Maria Martin:** Writing – review & editing, Methodology, Funding acquisition, Conceptualization. **Veronica Santoro:** Writing – review & editing, Formal analysis, Data curation. **Luisella Celi:** Writing – review & editing, Supervision, Project administration, Methodology, Funding acquisition, Conceptualization.

Declaration of competing interest

The authors declare that they have no known competing financial interests or personal relationships that could have appeared to influence the work reported in this paper.

Data availability

Data will be made available on request.

References

Cade-Menun, B., 2005. Characterizing phosphorus in environmental and agricultural samples by 31P nuclear magnetic resonance spectroscopy. Talanta 66, 359–371. https://doi.org/10.1016/j.talanta.2004.12.024.

Cade-Menun, B.J., 2015. Improved peak identification in 31P-NMR spectra of environmental samples with a standardized method and peak library. Geoderma 257–258, 102–114. https://doi.org/10.1016/j.geoderma.2014.12.016.

Cade-Menun, B., Liu, C.W., 2014. Solution phosphorus-31 nuclear magnetic resonance spectroscopy of soils from 2005 to 2013: a review of sample preparation and experimental parameters. Soil Sci. Soc. Am. J. 78, 19–37. https://doi.org/10.2136/sssaj2013.05.0187dgs.

Cade-Menun, B.J., Preston, C.M., 1996. A comparison of soil extraction procedures for 31P NMR spectroscopy. Soil Sci. 161, 770–785. https://doi.org/10.1097/00010694-199611000-00006.

Celi, L., Barberis, E., 2005. Abiotic reactions of inositol phosphates in soil. In: Turner, B. L., Frossard, E., Baldwin, D.S. (Eds.), Organic Phosphorus in the Environment. CABI Publishing, Wallingford, UK, pp. 65–84.

Celi, L., Prati, M., Magnacca, G., Said-Pullicino, D., Langella, A., Colombo, C., 2020. Role of crystalline iron oxides on stabilization of inositol phosphates in soil. Geoderma 374, 114442. https://doi.org/10.1016/j.geoderma.2020.114442.

Celi, L., Said-Pullicino, D., Bol, R., Guggenberger, G., Kaiser, K., 2022. Interconnecting soil organic matter with nitrogen and phosphorus cycling. In: Yang, Y., Keiluweit, M., Senesi, N., Xing, B. (Eds.), Multi-Scale Biogeochemical Processes in Soil Ecosystems, 1st edn. Wiley, pp. 51–77.

Chen, S., Cade-Menun, B.J., Bainard, L.D., Ma, B.L., Hamel, C., 2021. The influence of long-term N and P fertilization on soil P forms and cycling in a wheat/fallow cropping system. Geoderma 404, 115274. https://doi.org/10.1016/j.geoderma.2021.115274.

Chen, Z., Perez, J.P.H., Smales, G.J., Liu, J., Xu, Y., Liu, F., Xu, R.K., Zhu, M.Q., 2024. Impact of organic phosphates on the structure and composition of short-range ordered iron nanophases. Nanoscale Adv. 6, 2656–2668. https://doi.org/10.1039/D3NA01045G.

Colocho Hurtarte, L.C., Santana Amorim, H.C., Kruse, J., Vogel, C., Leinweber, P., Guggenberger, G., 2020. A novel approach for the quantification of different inorganic and organic phosphorus compounds in environmental samples by P $L_{2,3}$-edge X-ray absorption near-edge structure (XANES) spectroscopy. Environ. Sci. Technol. 54, 2812–2820. https://doi.org/10.1021/acs.est.9b07018.

Darilek, J.L., Huang, B., Li, D.-C., Wang, Z.-G., Zhao, Y.-C., Sun, W.-X., Shi, X.-Z., 2010. Effect of land use conversion from rice paddies to vegetable fields on soil phosphorus fractions. Pedosphere 20, 137–145. https://doi.org/10.1016/S1002-0160(10)60001-X.

De Sena, A., Madramootoo, C.A., Whalen, J.K., Antille, D.L., Smith, E.G., 2022. Nucleic acids are a major pool of hydrolyzable organic phosphorus in arable organic soils of Southern Ontario. Canada. Biol. Fertil. Soils 58, 7–16. https://doi.org/10.1007/s00374-021-01603-y.

Doolette, A.L., Smernik, R.J., Dougherty, W.J., 2009. Spiking improved solution phosphorus-31 nuclear magnetic resonance identificaiton of soil phosphorus compounds. Soil Sci. Soc. Am. J. 73, 919–927. https://doi.org/10.2136/sssaj2008.0192.

Duersch, B.G., Bhadha, J.H., Root, T.L., Louda, J.W., 2020. The role of rice (Oryza sativa L.) in sequestering phosphorus compounds and trace elements: Speciation and dynamics. Sci. Total Environ. 725, 138366. https://doi.org/10.1016/j.scitotenv.2020.138366.

Eivazi, F., Tabatabai, M.A., 1977. Phosphatases in soils. Soil Biol. Biochem. 9, 167–172. https://doi.org/10.1016/0038-0717(77)90070-0.

Frossard, E., Condron, L.M., Oberson, A., Sinaj, S., Fardeau, J.C., 2000. Processes governing phosphorus availability in temperate soils. J. Environ. Qual. 29, 15–23. https://doi.org/10.2134/jeq2000.00472425002900010003x.

Giaveno, C., Celi, L., Cessa, R.M.A., Prati, M., Bonifacio, E., Barberis, E., 2008. Interaction of organic phosphorus with clays extracted from Oxisols. Soil Sci. 173, 694–706. https://doi.org/10.1097/SS.0b013e3181893b59.

Giaveno, C., Celi, L., Richardson, A.E., Simpson, R.J., Barberis, E., 2010. Interaction of phytases with min and availability of substrate affect the hydrolysis of inositol phosphates. Soil Biol. Biochem. 42, 491–498. https://doi.org/10.1016/j.soilbio.2009.12.002.

Heiberg, L., Pedersen, T.V., Jensen, H.S., Kjaergaard, C., Bruun Hansen, H.C., 2010. A comparative study of phosphate sorption in lowland soils under oxic and anoxic conditions. J. Environ. Qual. 39, 734–743. https://doi.org/10.2134/jeq2009.0222.

Hofmann, K., Heuck, C., Spohn, M., 2016. Phosphorus resorption by young beech trees and soil phosphatase activity as dependent on phosphorus availability. Oecologia 181, 369–379.

Huang, X., Jiang, H., Li, Y., Ma, Y., Tang, H., Ran, W., Shen, Q., 2016. The role of poorly crystalline iron oxides in the stability of soil aggregate-associated organic carbon in a rice–wheat cropping system. Geoderma 279, 1–10. https://doi.org/10.1016/j.geoderma.2016.05.011.

IUSS Working Group WRB, 2022. World Reference Base for Soil Resources. International Soil Classification System For Naming Soils And Creating Legends For Soil Maps, 4th edition. International Union of Soil Sciences (IUSS), Vienna, Austria.

Kögel-Knabner, I., Amelung, W., Cao, Z., Fiedler, S., Frenzel, P., Jahn, R., Kalbitz, K., Kölbi, A., Schloter, M., 2010. Biogeochemistry of paddy soils. Geoderma 157, 1–14. https://doi.org/10.1016/j.geoderma.2010.03.009.

Kraal, P., Van Genuchten, C.M., Behrends, T., Rose, A.L., 2019. Sorption of phosphate and silicate alters dissolution kinetics of poorly crystalline iron (oxyhydr)oxide. Chemosphere 234, 690–701. https://doi.org/10.1016/j.chemosphere.2019.06.071.

Lane, J.M., Delavaux, C.S., Van Koppen, L., et al., 2022. Soil sample storage conditions impact extracellular enzyme activity and bacterial amplicon diversity metrics in a semi-arid ecosystem. Soil Biol. Biochem. 175, 108858. https://doi.org/10.1016/j.soilbio.2022.108858.

Liu, J., Cade-Menun, B.J., Yang, J., Hu, Y.F., Liu, C.W., Tremblay, J., LaForge, K., Schellenberg, M., Hamel, C., Bainard, L.D., 2018. Long-term land use affects

phosphorus speciation and the composition of phosphorus cycling genes in agricultural soils. Front. Microbiol. 9, 1643. https://doi.org/10.3389/fmicb.2018.01643.
Lizcano Toledo, R., Lerda, C., Moretti, B., Miniotti, E., Santoro, V., Fernandez-Ondoño, E., Martin, M., Said-Pullicino, D., Romani, M., Celi, L., 2022. Cover crops increase N and P cycling and rice productivity in temperate cropping systems. Agronomy 12, 2193.
Marschner, P., 2021. Processes in submerged soils – linking redox potential, soil organic matter turnover and plants to nutrient cycling. Plant Soil 464, 1–12. https://doi.org/10.1007/s11104-021-05040-6.
Martin, M., Celi, L., Barberis, E., 1999. Determination of low concentrations of organic phosphorus in soil solution. Commun. Soil Sci. Plant Anal. 30, 1909–1917. https://doi.org/10.1080/00103629909370341.
Martinengo, S., Schiavon, M., Santoro, V., Celi, L., Said-Pullicino, D., Prietzel, J., Oberson, A., Frossard, E., 2023. Assessing phosphorus availability in paddy soils: the importance of integrating soil tests and plant responses. Biol. Fertil. Soils 59, 391–405. https://doi.org/10.1007/s00374-023-01714-8.
Martinengo, S., Santoro, V., Schiavon, M., Celi, L., Martin, M., Said-Pullicino, D., 2024. The influence of phosphorus availability on rice root traits driving iron plaque formation and dissolution, and implications for phosphorus uptake. Plant Soil 494, 603–616. https://doi.org/10.1007/s11104-023-06306-x.
Miniotti, E.F., Romani, M., Said-Pullicino, D., Bertora, C., Sacco, D., 2016. Agro-environmental sustainability of different water management practices in temperate rice agro-ecosystems. Agric. Ecosyst. Environ. 222, 235–248. https://doi.org/10.1016/j.agee.2016.02.010.
Moody, P.W., Speirs, S.D., Scott, B.J., Mason, S.D., 2013. Soil phosphorus tests I: what soil phosphorus pools and processes do they measure? Crop Pasture Sci. 64, 461. https://doi.org/10.1071/CP13112.
Murphy, J., Riley, J.P., 1962. A modified single solution method for the determination of phosphate in natural waters. Anal. Chim. Acta 27, 31–36. https://doi.org/10.1016/S0003-2670(00)88444-5.
Olsen, S.R., Sommers, L.E., 1982. Phosphorus. Agronomy 9. In: Page, A.L., Miller, R.H., Keeney, D.R. (Eds.), Methods of Soil Analysis, Part 2, 2nd edn. ASA, Madison, WI, pp. 403–430.
Peng, Y., Duan, Y., Huo, W., Zhang, Y., Liu, Y., Wang, Y., Zhang, X., 2021. Soil microbial biomass phosphorus can serve as an index to reflect soil phosphorus fertility. Biol. Fertil. Soils 57, 657–669. https://doi.org/10.1007/s00374-021-01559-z.
Peoples, M.S., Koide, R.T., 2012. Considerations in the storage of soil samples for enzyme activity analysis. Appl. Soil Ecol. 62, 98–102. https://doi.org/10.1016/j.apsoil.2012.08.002.
Ponnamperuma, F.N., 1972. The chemistry of submerged soils. In: Advances in Agronomy. Elsevier, pp. 29–96.
Prietzel, J., Harrington, G., Häusler, W., Heuck, C., Spohn, M., 2016. Reference spectra of important adsorbed organic and inorganic phosphate binding forms for soil P speciation using synchrotron-based K-edge XANES spectroscopy. J. Synchrotron Radiat. 23, 532–544. https://doi.org/10.1107/S1600577515023085.
R Core Team, 2021. R: a language and environment for statistical computing. R Foundation for Statistical Computing, Vienna, Austria https://www.R-project.org/.
Raiesi, F., Beheshti, A., 2014. Soil specific enzyme activity shows more clearly soil responses to paddy rice cultivation than absolute enzyme activity in primary forests of northwest Iran. Appl. Soil Ecol. 75, 63–70. https://doi.org/10.1016/j.apsoil.2013.10.012.
Recena, R., Cade-Menun, B.J., Delgado, A., 2018. Organic phosphorus forms in agricultural soils under Mediterranean climate. Soil Sci. Soc. Am. J. 82, 783–795. https://doi.org/10.2136/sssaj2017.10.0360.
Refait, P., Reffass, M., Landoulsi, J., Génin, J.M.R., 2007. Role of phosphate species during the formation and transformation of the Fe(II–III) hydroxycarbonate green rust. Colloids Surf. Physicochem. Eng. Asp. 299, 29–37. https://doi.org/10.1016/j.colsurfa.2006.11.013.
Richardson, A.E., Hocking, P.J., Simpson, R.J., George, T.S., 2009. Plant mechanisms to optimize access to soil phosphorus. Crop Pasture Sci. 60, 124. https://doi.org/10.1071/CP07125.
Rose, T.J., Impa, S.M., Rose, M.T., Pariasca-Tanaka, J., Mori, A., Heuer, S., Wissuwa, M., 2013. Enhancing phosphorus and zinc acquisition efficiency in rice: a critical review of root traits and their potential utility in rice breeding. Ann. Bot. 112, 331–345. https://doi.org/10.1093/aob/mcs217.
Saggar, S., Hedley, M.J., White, R.E., 1990. A simplified resin membrane technique for extracting phosphorus from soils. Fertil. Res. 24, 173–180. https://doi.org/10.1007/BF01073586.
Santoro, V., Martin, M., Persson, P., Celi, L., 2019. Inorganic and organic P retention by coprecipitation during ferrous iron oxidation. Geoderma 348, 168–180. https://doi.org/10.1016/j.geoderma.2019.04.004.
Santoro, V., Schiavon, M., Celi, L., 2023. Role of soil abiotic processes on phosphorus availability and plant responses with a focus on strigolactones in tomato plants. Plant Soil. https://doi.org/10.1007/s11104-023-06266-2.
Scalenghe, R., Edwards, A.C., Ajmone Marsan, F., Barberis, E., 2002. The effect of reducing conditions on the solubility of phosphorus in a diverse range of European agricultural soils: Redox conditions and P solubility. Eur. J. Soil Sci. 53, 439–447. https://doi.org/10.1046/j.1365-2389.2002.00462.x.
Schwertmann, U., 1964. Differenzierung der Eisenoxide des Bodens durch Extraktion mit Ammoniumoxalat-Lösung. Z. Pflanzenernähr. Düng. Bodenkd. 105, 194–202. https://doi.org/10.1002/jpln.3591050303.
Senn, A.-C., Kaegi, R., Hug, S.J., Hering, J.G., Mangold, S., Wehrli, B., 2015. Composition and structure of Fe(III)-precipitates formed by Fe(II) oxidation in water at near-neutral pH: Interdependent effects of phosphate, silicate and Ca. Geochim. Cosmochim. Acta 162, 220–246. https://doi.org/10.1016/j.gca.2015.04.032.
Sodano, M., Lerda, C., Nisticò, R., Said-Pullicino, D., Celi, L., 2017. Dissolved organic carbon retention by coprecipitation during the oxidation of ferrous iron. Geoderma 307, 19–29. https://doi.org/10.1016/j.geoderma.2017.07.022.
Solangi, F., Zhu, X., Khan, S., Rais, N., Majeed, A., Sabir, M.A., Iqbal, R., Ali, S., Hafeez, A., Ali, B., Ercisli, S., Kayabasi, E.T., 2023. The global dilemma of soil legacy phosphorus and its improvement strategies under recent changes in agro-ecosystem sustainability. ACS Omega 8, 23271–23282. https://doi.org/10.1021/acsomega.3c00823.
Soltanpour, P.N., Adams, F., Bennett, A.C., 1974. Soil phosphorus availability as measured by displaced soil solutions, calcium-chloride extracts, dilute-acid extracts, and labile phosphorus. Soil Sci. Soc. Am. J. 38, 225–228. https://doi.org/10.2136/sssaj1974.03615995003800020010x.
Sposito, G., 2008. The Chemistry of Soils, 2nd edn. Oxford University Press, Oxford.
Trasar-Cepeda, C., Leirós, M.C., Gil-Sotres, F., 2008. Hydrolytic enzyme activities in agricultural and forest soils. some implications for their use as indicators of soil quality. Soil Biol. Biochem. 40, 2146–2155. https://doi.org/10.1016/j.soilbio.2008.03.015.
Turner, B.L., 2008. Soil organic phosphorus in tropical forests: an assessment of the NaOH–EDTA extraction procedure for quantitative analysis by solution 31P NMR spectroscopy. Eur. J. Soil Sci. 59, 453–466. https://doi.org/10.1111/j.1365-2389.2007.00994.x.
Turner, B.L., Cade-Menun, B.J., Condron, L.M., Newman, S., 2005. Extraction of soil organic phosphorus. Talanta 66, 294–306. https://doi.org/10.1016/j.talanta.2004.11.012.
Turner, B.L., Cheesman, A.W., Godage, H.Y., Riley, A.M., Potter, B.V.L., 2012. Determination of neo- and D-chiro-inositol hexakisphosphate in soils by solution 31P NMR spectroscopy. Environ. Sci. Technol. 46, 4994–5002. https://doi.org/10.1021/es204446z.
Wang, C., Dippold, M.A., Kuzyakov, Y., Dorodnikov, M., 2024. Microbial strategies for phosphorus acquisition in rice paddies under contrasting water regimes: Multiple source tracing by 32P and 33P. Sci. Total Environ. 918, 170738. https://doi.org/10.1016/j.scitotenv.2024.170738.
Wang, C., Thielemann, L., Dippold, M.A., Kuzyakov, Y., Dorodnikov, M., 2022a. Can the reductive dissolution of ferric iron in paddy soils compensate phosphorus limitation of rice plants and microorganisms? Soil Biol. Biochem. 168, 108653. https://doi.org/10.1016/j.soilbio.2022.108653.
Wang, C., Thielemann, L., Dippold, M.A., Kuzyakov, Y., Dorodnikov, M., 2022b. Microbial iron reduction compensates for phosphorus limitation in paddy soils. Sci. Total Environ. 837, 155810. https://doi.org/10.1016/j.scitotenv.2022.155810.
Wang, X., Hu, Y., Tang, Y., Li, H., Yang, P., Wang, S., Jin, Z., 2017. Phosphate and phytate adsorption and precipitation on ferrihydrite surfaces. Environ. Sci. Nano 4, 2193–2204. https://doi.org/10.1039/C7EN00705A.
Wu, G., Wei, K., Chen, Z., Zhang, Y., Liu, J., Wang, Y., Zhang, X., 2021. Crop residue application at low rates could improve soil phosphorus cycling under long-term no-tillage management. Biol. Fertil. Soils 57, 499–511. https://doi.org/10.1007/s00374-020-01531-3.
Zampieri, M., Ceglar, A., Dentener, F., Toreti, A., 2019. When will current climate extremes affecting maize production become the norm? Earth's Future 7, 113–122. https://doi.org/10.1029/2018EF000995.
Zhang, Y., Lin, X., Werner, W., 2003. The effect of soil flooding on the transformation of Fe oxides and the adsorption/desorption behavior of phosphate. J. Plant Nutr. Soil Sci. 166, 68–75. https://doi.org/10.1002/jpln.200390014.
Zhang, Z., Xie, D., Teng, W., Gu, F., Zhang, R., Cheng, K., Liu, Z., Zhao, Y., Yang, F., 2025. A state of art review on carbon, nitrogen, and phosphorus cycling and efficient utilization in paddy fields. Plant and Soil. https://doi.org/10.1007/s11104-025-07344-3.
Zhu, Y., Wu, F., He, Z., Guo, J., Qu, X., Xie, F., Giesy, J.P., Liao, H., Guo, F., 2013. Characterization of organic phosphorus in lake sediments by sequential fractionation and enzymatic hydrolysis. Environ. Sci. Technol. 47, 7679–7686. https://doi.org/10.1021/es305277g.
Zhu, J., Li, M., Whelan, M., 2018. Phosphorus activators contribute to legacy phosphorus availability in agricultural soils: a review. Sci. Total Environ. 612, 522–537. https://doi.org/10.1016/j.scitotenv.2017.08.095.